

THE NATURE OF THE NUCLEON-NUCLEON  
INTERACTION IN THE QUARK MODEL\*

A. FAESSLER

University of Tuebingen, Institute of Theoretical Physics  
Auf der Morgenstelle 14, 72076 Tuebingen, Germany*(Received November 24, 1997)*

The nucleon-nucleon interaction is studied in the Tuebingen Chiral Quark model. The quark-quark hamiltonian includes, in addition to a quadratic confinement potential and the usual one-gluon exchange, pion and sigma exchanges between quarks generated by chiral symmetry breaking. An expansion up to second order in  $v/c$  is used. The requirement of chiral symmetry reduces the number of free parameters in the model. The  $\sigma$  meson is exchanged between quarks and not as in earlier versions between nucleons. Within the model the nucleon-nucleon phase shifts and the deuteron properties are studied. The longitudinal and transversal form factors of the deuteron are calculated in this microscopic meson-quark cluster model.

PACS numbers: 21.30. Cb, 21.30. Fe

**1. Introduction**

The first idea about the nature of the nucleon-nucleon interaction came from Yukawa in 1935. He assumed that the strong interaction between two nucleons is carried by an interaction quantum, which is a particle of a medium heavy mass of about 200 MeV, the meson. After finding the  $\pi$  meson one thought one has found the carrier of the strong nuclear force. But the fifties saw a time where more and more mesons were found which contribute to the nucleon-nucleon interaction. One of the high points of this development was the suggestion of Gregory Breit in 1958 that the short range repulsion should be due to a vector, isoscalar meson, the omega meson ( $\omega$ ) with a mass of about 800 MeV. It was a big success of the meson exchange theory of the nucleon-nucleon interaction when this  $\omega$  meson was found also experimentally.

---

\* Presented at the XXV Mazurian Lakes School of Physics, Piaski, Poland, August 27-September 6, 1997.

But just the  $\omega$  meson shows that this cannot be the whole story. Flavor symmetry  $SU(3)$  predicts from the  $\rho$ -nucleon coupling the  $\omega$ -nucleon coupling squared  $g_{\omega NN}^2/(4\pi) = 4.5$ . In reality one needs to reproduce the short repulsion according to the Bonn-potential values between 12 and 24. Normally flavor  $SU(3)$  is only violated within 30 % or less. The need to blow up the square of the  $\omega - NN$  coupling constant by a factor 2 and more indicates that the  $\omega$  meson must carry a load for which it is not prepared. After we learned that the nucleon is composed out of three valence quarks, gluons and sea quarks it is natural to look on the quark level for the nature of the short range repulsion. Indeed we will show in the next chapter that the short range repulsion of the  $NN$  interaction can be understood in the quark model by the symmetry of the 6-valence quarks [1–7]. The main purpose of this work is to search for quark degrees of freedom in the deuteron properties and in the nucleon–nucleon ( $NN$ ) interaction.

In the second chapter we extend the quark cluster model to include chiral symmetry, which is broken afterwards by quark condensates [8–15]. This connects the sigma meson quark coupling constant to the pion–nucleon coupling. PCAC gives a relation [16] between the sigma meson mass and the pion and quark masses. In this way the number of parameters can be drastically reduced. Furthermore one does not need to have two different values for the quark-sigma meson (or nucleon-sigma meson) coupling for S and higher partial waves [10–13].

In the third chapter we calculate the deuteron wave function in the quark cluster model. For the electromagnetic deuteron form factors of the elastic electron deuteron scattering we include the impulse term where the photon is directly interacting with the quarks and exchange currents [17–20].

## 2. The quark model and the nn interaction

At large distances the nucleon-nucleon interaction can be represented quite successfully by exchanging mesons between the centre of mass of nucleon 1 and the centre of mass of nucleon 2. At smaller distances it makes no sense to exchange mesons between the centre of mass of the two nucleons, since due to antisymmetrization it is not even known where the centre of masses of the two nucleons are, since the antisymmetrizer attaches the 6-valence quarks in each of the ten terms of the antisymmetrization to other nucleons. The difficulty of the meson exchange model at short distances might be indicated by the too large  $\omega - NN$  coupling constant needed to reproduce the data as indicated in the introduction. At short distances (below 1 fm), where the quark contents of the two nucleons overlap, the quark degrees of freedom should play a major role in describing the nucleon–nucleon ( $NN$ ) interaction and especially the short range repulsion.

In principle we should describe the NN interaction by quantum chromodynamics (QCD). But QCD is highly nonperturbative. This shows up in the color confinement phenomenon at large distances and the appearance of chiral condensates  $\langle \bar{\psi} \psi \rangle \neq 0$  of quarks which break chiral symmetry. As a consequence of chiral symmetry breaking current quarks acquire a constituent mass  $m_q = m_N/3 \approx 330$  MeV. This symmetry breaking only occurs at small momenta  $|q| < \Lambda_{\text{CSB}}$ . These ideas have been included by Shuryak [8] into an instanton liquid model of QCD. Using this picture Diakonov [9] derived an effective low-momentum Lagrangian,

$$L_{\text{QCD}} = \bar{\psi}_f^\alpha (i\gamma^\beta \partial_\beta - m(q^2) e^{i\gamma_5} (\vec{\pi} \cdot \vec{\tau}) \psi_f^\alpha. \quad (1)$$

Here  $\bar{\psi}_f^\alpha$  is the quark spinor with color  $\alpha$  and flavor  $f, f'$ .  $m(q^2)$  is the dynamical mass of the quarks.

From Eq. (1) one can derive the effective interaction between quarks and pions and its chiral partner the  $\sigma$  meson:

$$H_{\text{chiral}} = m(q^2) \bar{\psi} \exp \left( \frac{i\gamma_5 \vec{\tau} \cdot \vec{\phi}}{f_\phi} \right) \psi. \quad (2)$$

If one linearizes this expression using,

$$\begin{aligned} \pi &= \vec{\phi} f_\pi \sin(\phi/f_\pi), \\ \sigma &= f_\pi [\cos(\phi/f_\pi) - 1] \end{aligned} \quad (3)$$

one obtains:

$$H_{\text{chiral}} = g_{ch} F(q^2) \bar{\psi} (\sigma + i\gamma_5 \vec{\tau} \cdot \vec{\pi}) \psi, \quad (4)$$

where  $g_{ch} = m_q(0)/f_\pi$ ,  $F(q^2) = m_q(q^2)/m_q(0)$ . This expression differs from the Hamiltonian in the linear  $\sigma$ -model in the modification of the coupling constant  $g_{ch}$  by the form factor  $F(q^2)$ ,

$$F(q^2) = \left[ \frac{\Lambda_{\text{CSB}}^2}{\Lambda_{\text{CSB}}^2 + q^2} \right]^{1/2}. \quad (5)$$

This allows us now to write down the potential generated between quark  $i$  and  $j$  by the exchange of  $\pi$  and  $\sigma$  mesons [10–13, 22],

$$\begin{aligned} V_{\text{OPE}}(\vec{r}_{ij}) &= \frac{1}{3} \alpha_{ch} \frac{\Lambda^2}{\Lambda^2 - m_\pi^2} m_\pi \left\{ \left[ Y(m_\pi r_{ij}) - \frac{\Lambda^3}{m_\pi^3} Y(\Lambda r_{ij}) \right] \vec{\sigma}_i \cdot \vec{\sigma}_j + \right. \\ &\quad \left. \left[ H(m_\pi r_{ij}) - \frac{\Lambda^3}{m_\pi^3} H(\Lambda r_{ij}) \right] S_{ij} \right\} \vec{\tau}_i \cdot \vec{\tau}_j, \end{aligned} \quad (6)$$

$$V_{\text{OSE}}(\vec{r}_{ij}) = -\alpha_{ch} \frac{4m_q^2}{m_\pi^2} \frac{\Lambda^2}{\Lambda^2 - m_\sigma^2} m_\sigma \left[ Y(m_\sigma r_{ij}) - \frac{\Lambda}{m_\sigma} Y(\Lambda r_{ij}) \right], \quad (7)$$

Here  $\alpha_{ch}$  is the chiral coupling constant.  $r_{ij}$  is the interquark distance.  $S_{ij}$  is the quark tensor operator,

$$S_{ij} = 3(\vec{\sigma}_i \cdot \hat{r}_{ij})(\vec{\sigma}_j \cdot \hat{r}_{ij}) - \vec{\sigma}_i \cdot \vec{\sigma}_j, \quad (8)$$

$Y(x)$  and  $H(x)$  being the Yukawa functions defined as,

$$Y(x) = \frac{e^{-x}}{x}, \quad H(x) = \left(1 + \frac{3}{x} + \frac{3}{x^2}\right) Y(x). \quad (9)$$

The scale for chiral symmetry breaking must lie between 1 GeV and 600 MeV to reproduce the adequate cut-off for the instanton fluctuations [8], we chose 829 MeV. In addition to the  $\pi$  and  $\sigma$  exchange between quarks one introduces in the quark cluster model confinement,

$$V_{\text{con}}(\vec{r}_{ij}) = -a_c (\vec{\lambda}_i \cdot \vec{\lambda}_j) r_{ij}^2, \quad (10)$$

and the one gluon exchange potential,

$$V_{\text{OGE}}(\vec{r}_{ij}) = \frac{1}{4} \alpha_s \vec{\lambda}_i \cdot \vec{\lambda}_j \left\{ \frac{1}{r_{ij}} - \frac{\pi}{m_q^2} \left[ 1 + \frac{2}{3} \vec{\sigma}_i \cdot \vec{\sigma}_j \right] \delta(\vec{r}_{ij}) - \frac{3}{4m_q^2 r_{ij}^3} S_{ij} + \text{two-body spin-orbit} \right\}. \quad (11)$$

Here  $\vec{\lambda}_i$  are the eight color octet matrices acting on quark  $i$ . The two body spin-orbit contribution is not written down. It plays an important role in higher ( $L \neq 0$ ) partial waves. The total Hamiltonian of the quark cluster model has, with chirally invariant quark-pion and quark-sigma interaction for the six quarks of two baryons, the form:

$$H_{\text{quark}} = \sum_{i=1}^6 \left[ m_i + \frac{\vec{p}_i^2}{2m_i} \right] - T_{\text{C.M.}} + \sum_{i < j=1}^6 [V_{\text{OGE}}(\vec{r}_{ij}) + V_{\text{OPE}}(\vec{r}_{ij}) + V_{\text{OSE}}(\vec{r}_{ij}) + V_{\text{con}}(\vec{r}_{ij})]. \quad (12)$$

The quark mass is taken to be  $m_q = 313$  MeV. It is essentially  $m_N/3 = m_q$ . The oscillator length is determined to fit, with the pion cloud around the nucleon the electric proton root mean square radius  $\langle r^2 \rangle^{1/2} = 0.83$  fm

[21].  $\alpha_{ch}$  can be connected with the experimental pion–nucleon coupling constant [10]

$$\alpha_{ch} = \left(\frac{3}{5}\right)^2 \frac{g_{\pi NN}^2}{4\pi} \frac{m_\pi^2}{4M_N^2}. \quad (13)$$

For the mass of the  $\sigma$  meson PCAC provides a relation [16]

$$m_\sigma^2 = (2m_q)^2 + m_\pi^2. \quad (14)$$

If one fixes the pion mass by the physical value, one obtains a value for  $m_\sigma$  between 650 and 700 MeV. We chose 675 MeV. The cut off mass for chiral symmetry breaking can be related to the cut off mass in the pion–nucleon form factor [10]

Figs 1 and 2 show the results for the  $^1S_0$  and the  $^3S_1$  NN phase shifts. For the  $^1S_0$  phase shift the coupling to the  $^5D_0$   $N\Delta$  channel is essential [22]. Figures 3 to 12 show the higher partial waves apart  $^3F_2$  and  $^3F_3$  where the  $^5F_2$ ,  $^5P_2$ ,  $^7F_2$ ,  $^7P_2$ ,  $^7H_2$  and  $^5F_3$ ,  $^5P_3$ ,  $^5H_3$ ,  $^7F_3$ ,  $^7P_3$  and  $^7H_3$  partial waves of the  $N\Delta$  and  $\Delta\Delta$  channels play an important role, which we want to include in the future. The quark cluster model explains also nicely the short range repulsion of the nucleon–nucleon interaction [1, 2].

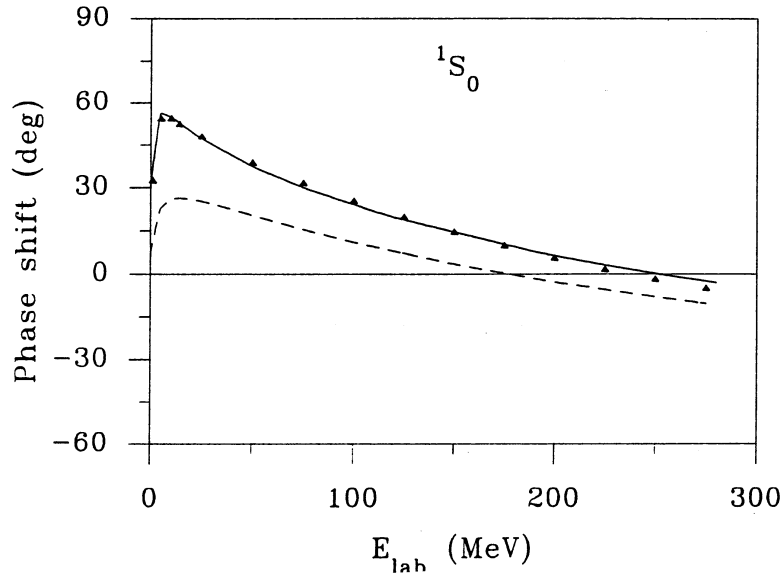


Fig.1. Singlet  $^1S_0$  NN phase shift including chiral symmetry and coupling to the  $^5D_0$   $N\Delta$  channel (solid line). The dots are the experimental phase shifts [23]. The dashed line is the result without the inclusion of the  $^5D_0$   $N\Delta$  channel.

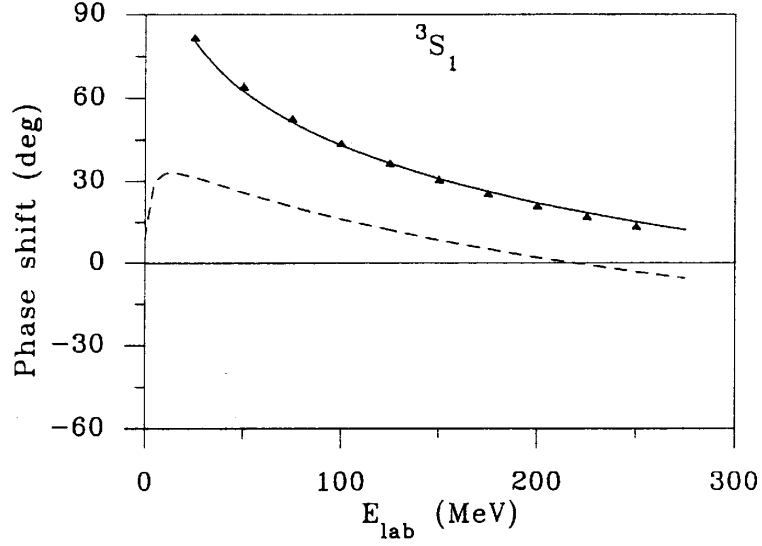


Fig. 2.  ${}^3S_1 NN$  phase shift. The dots are the experimental values [23]. The solid line is the result of the present model calculation including chiral symmetry. The dashed curve is the result without coupling to the  ${}^3D_1 NN$  partial wave.

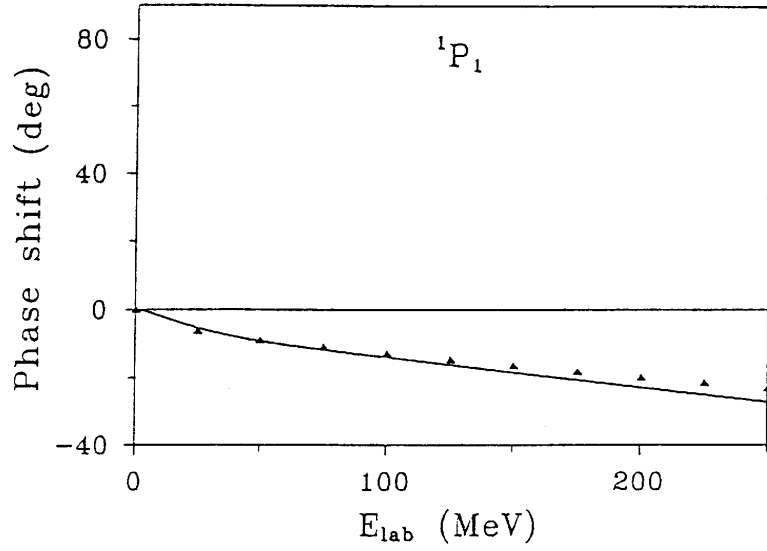


Fig. 3. Phase shift of the  ${}^1P_1$  partial wave with the parameters given in Table I compared with the data.

TABLE I

The parameters

$m_q$ MeV	$b$ fm	$\alpha_s$	$g_{\pi NN}^2/4\pi$	$a_c$ MeV · fm <sup>-2</sup>	$m_\sigma$ fm <sup>-1</sup>	$\Lambda_{\text{CSB}}$ fm <sup>-1</sup>
313	0.518	0.485	13.7	46.94	3.42	4.2

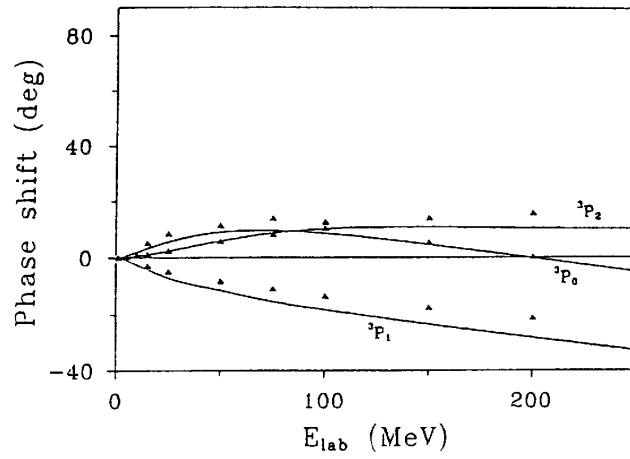


Fig. 4. Phase shifts of the  $^3P_0$ ,  $^3P_1$  and  $^3P_2$  partial waves of the nucleon–nucleon interaction as a function to the laboratory bombarding energy compared with the data.

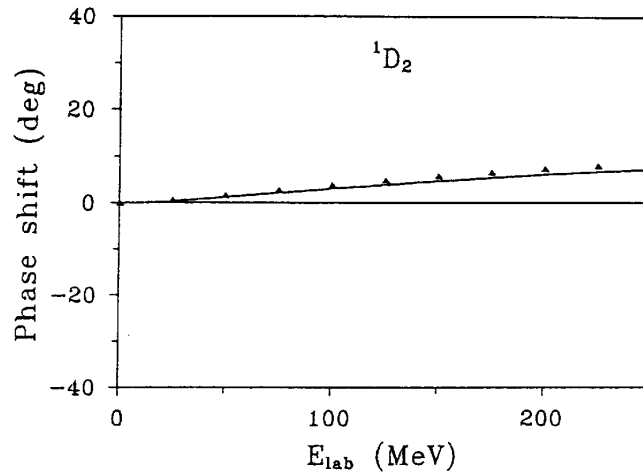


Fig. 5. Phase shift of the  $^1D_2$  partial wave.

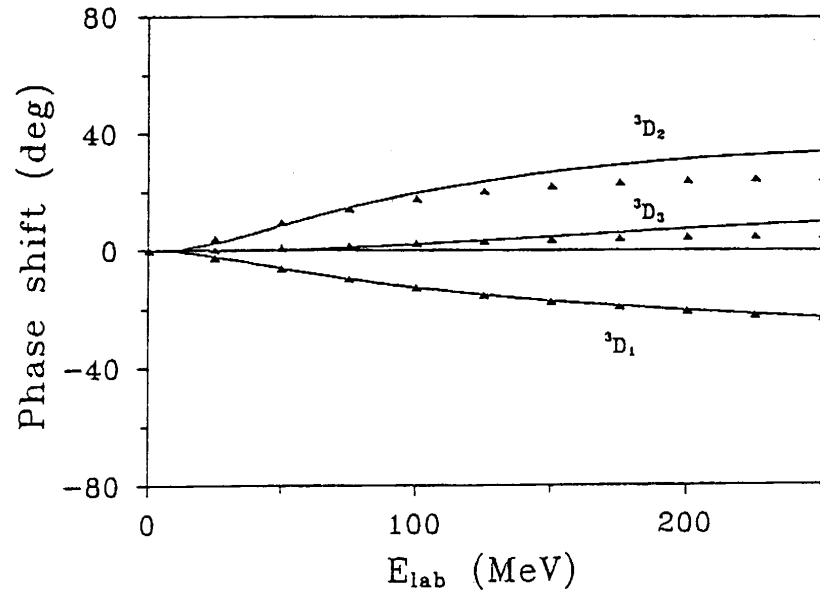


Fig. 6. Phase shifts of the  ${}^3D_J$  ( $J = 1, 2, 3$ ) partial waves.

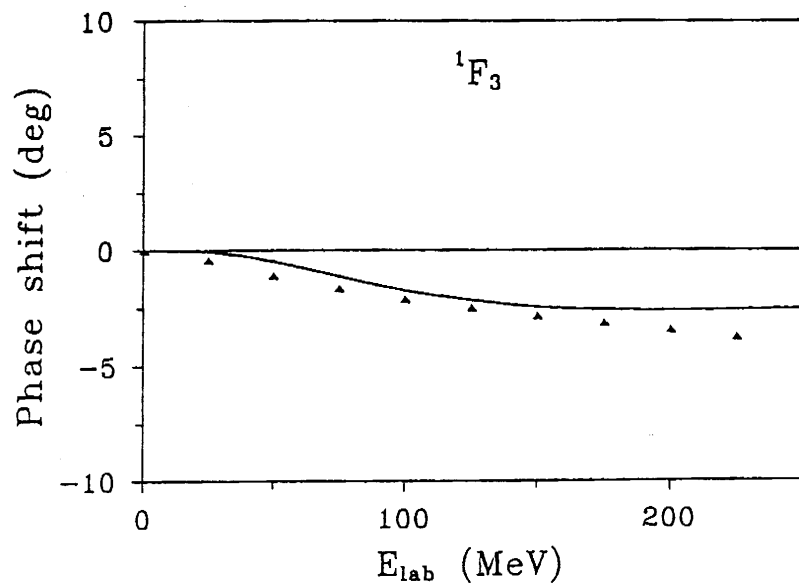


Fig. 7. Phase shift of the  ${}^1F_3$  partial wave.



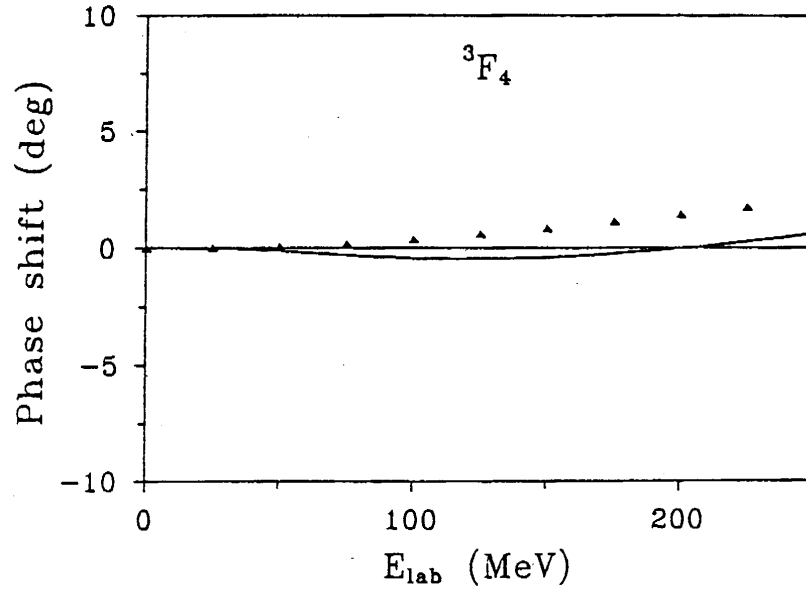


Fig. 8. Phase shift of the  ${}^3F_4$  partial wave.

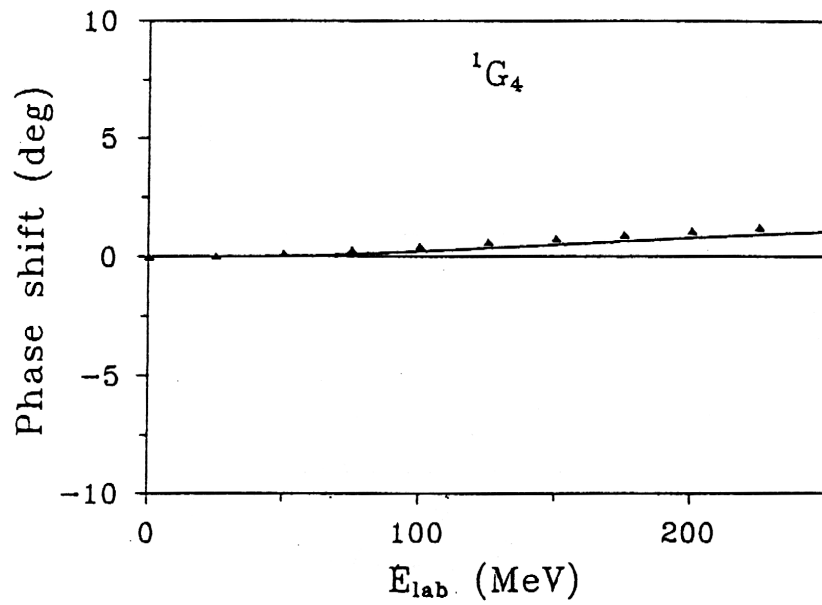


Fig. 9. Phase shift of the  ${}^1G_4$  partial wave.

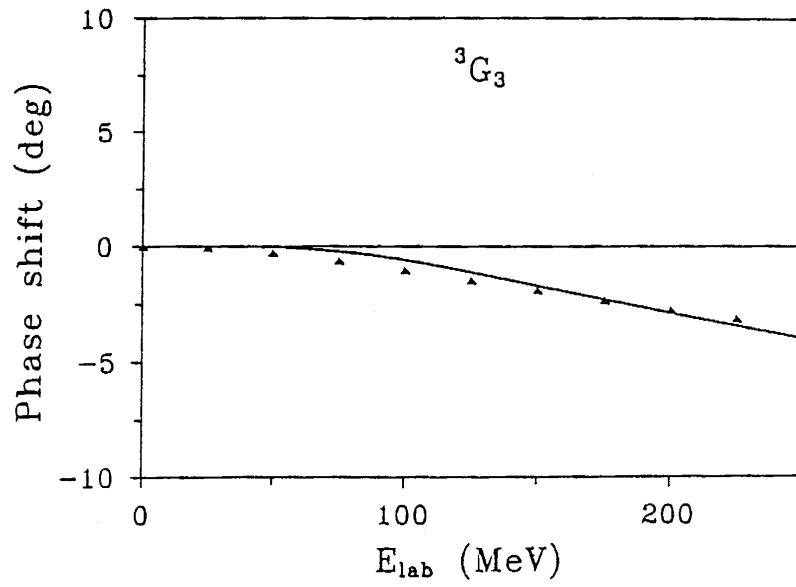


Fig. 10. Phase shift of the  ${}^3G_3$  partial wave.

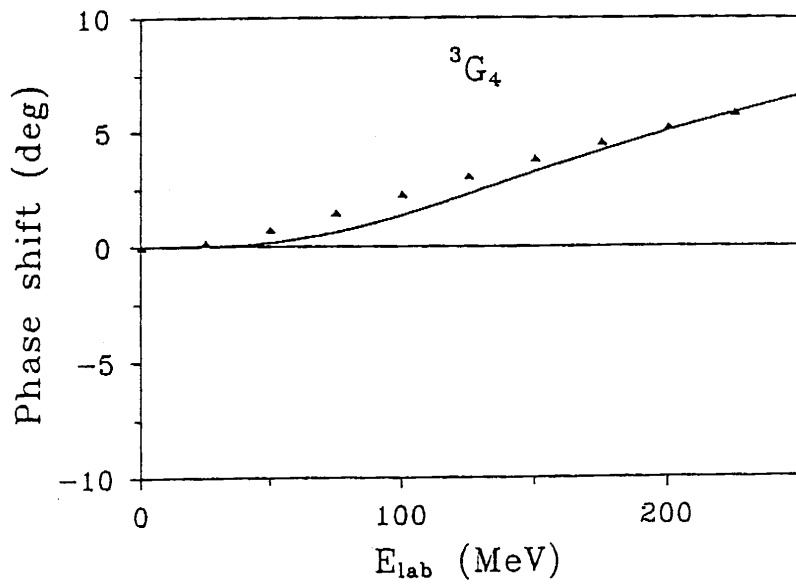


Fig. 11. Phase shift of the  ${}^3G_4$  partial wave.

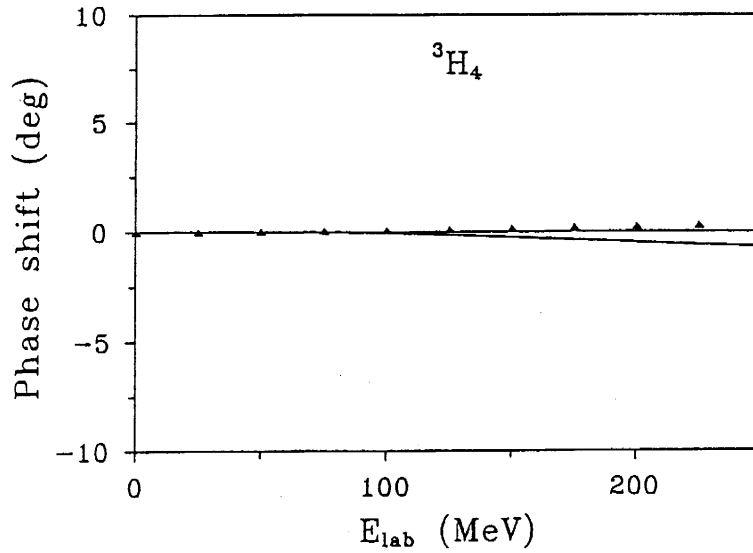


Fig. 12. Phase shift of the  ${}^3H_4$  partial wave compared with the data.

Fig. 13 shows the spatial symmetries of the 6-quarks at small distances.

$$\begin{array}{c}
 \mathcal{A} \left\{ \begin{array}{c} \text{Two nucleons at distance } r \\ \text{Each nucleon has 3 quarks in } 1s \text{ state} \end{array} \right\} = \frac{1}{9} \begin{array}{c} \text{Six quarks in } 1s \text{ state at } r=0 \\ \text{Completely symmetric} \end{array} + \frac{8}{9} \begin{array}{c} \text{Six quarks in } 1s \text{ state at } r=0 \\ \text{[42] symmetry} \end{array} \\
 \\
 \begin{array}{c} \boxed{\phantom{0}} \boxed{\phantom{0}} \boxed{\phantom{0}} \times \boxed{\phantom{0}} \boxed{\phantom{0}} \boxed{\phantom{0}} = \frac{1}{9} \boxed{\phantom{0}} \boxed{\phantom{0}} \boxed{\phantom{0}} \boxed{\phantom{0}} \boxed{\phantom{0}} \boxed{\phantom{0}} + \frac{8}{9} \begin{array}{c} \boxed{\phantom{0}} \boxed{\phantom{0}} \boxed{\phantom{0}} \boxed{\phantom{0}} \\ \boxed{\phantom{0}} \boxed{\phantom{0}} \end{array} \\
 \\
 (3)_r \times (3)_r = \frac{1}{9} (6)_r + \frac{8}{9} (4\ 2)_r
 \end{array}$$

Fig. 13. The left hand side shows two nucleons in the quark model at distance  $r$ . In each of the two nucleons all three valence quarks are in the  $1s$  state. Group theory tells us that if the two nucleons are in a relative orbital  $S$ -state. The permutation symmetry of all 6 valence quarks can either be only completely symmetric  $[6]$  or have the  $[42]$  symmetry. The square of the Clebsch–Gordan coefficients of the permutation group of 6 objects gives also the probability to find the completely symmetric spatial representation  $[6]$  or the  $[42]$  symmetry.

One sees that it is more probable by the weight  $8/9$  to have at short distance the  $[42]$  symmetry compared with the completely symmetric orbital wave function  $[6]$  which has only the weight  $1/9$ . Fig. 13 indicates also the lowest energy realizations of the orbital symmetries  $[6]$  and the mixed orbital symmetry  $[42]$ . The last configuration requests at zero distance of the two nucleons ( $r = 0$ ) that two quarks are in the  $1p$  state for the lowest energy realization of this configuration. The usual way of representing the two nucleon wave function by 6 quarks in the  $1s$  state is only contained with the probability  $1/9$ . It is obvious that the  $[42]$  orbital symmetry cannot be neglected. If for a moment we neglect  $1/9$  compared to  $8/9$  we have at small distances  $r \approx 0$  at least two harmonic oscillator quanta excited. Or in other words at least two quarks have to be not in the  $1s$  state. For the lowest configuration they are in the  $1p$  state. That means at short distances this configuration with the probability  $8/9$  has at least two harmonic oscillator quanta excited. If one moves again the two nucleons apart at distance  $r$  as on the left hand side of Fig. 13, one sees that inside the two nucleons one has no harmonic oscillator quanta excited. Since one has to conserve the number of harmonic oscillator quanta, the two quanta must be contained in the relative motion. If one expands the relative  $S$  wave function of the two nucleons in harmonic oscillators

$$u(r_{12}) = \alpha_1|1s\rangle + \alpha_2|2s\rangle + \alpha_3|3s\rangle + \dots,$$

with :

$$\alpha_1 = 0, \quad (\text{Pauli forbidden}), \quad (15)$$

one finds that the  $1s$  amplitude must be zero since all parts of the wave function have to contain at least two harmonic oscillator quanta if one considers the orbital  $[42]$  symmetry. Thus the relative wave function  $u(r_{12})$  is dominated at small distances by  $|2s\rangle$  and therefore has a node near the so-called hardcore radius ( $r = 0.4$  fm). This node is seen in the asymptotic phase shift measured by the differential cross section. To explain the node one requests that the nucleon-nucleon interaction potential has a hard or soft core at this radius. In reality the node in the wave function is enforced by the orbital  $[42]$  symmetry.

### 3. Conclusions

In this contribution I have essentially communicated three messages:

- (i) A short range repulsion of the nucleon–nucleon interaction is not due to the hard or soft core in a static nucleon–nucleon potential but is due to many body symmetries of the 6-valence-quarks of the two interacting

nucleons. At short distances the spatial symmetry is of [42] nature with the probability  $8/9$ . This requests that one has at least two harmonic oscillator quanta in the relative wave function. That means one has a node in the interaction region which produces a hard core phase shift in the differential cross section.

- (ii) Inclusion of chiral symmetry allows to calculate the NN data without fitting any six quark data. For the  $^1S_0$  phase shift the  $^5D_0$   $N \Delta$  admixture plays an important role. The contribution of the two body spin-orbit force from gluon and  $\sigma$  exchange may add or subtract in different partial waves. This improves the description of the  $^3L_J$  (with  $J = L - 1, L$  and  $L + 1$ ) phase shifts without fitting the two-body spin-orbit strength.

I would like to thank Profs F. Fernández, Zhang Zong-ye and Drs A. Valcarce, A. Buchmann, L. Glozman, U. Straub and Y. Yamauchi with whom this work has been performed.

#### REFERENCES

- [1] A. Faessler, F. Fernández, G. Lübeck, K. Shimizu, *Phys. Lett.* **112B**, 201 (1982).
- [2] A. Faessler, F. Fernández, G. Lübeck, K. Shimizu, *Nucl. Phys.* **A402**, 555 (1983).
- [3] M. Oka, K. Yazaki, *Progr. Theor. Phys.* **66**, 556, 572 (1981).
- [4] M. Oka, K. Yazaki, *Quarks and Nuclei*, World Scientific, Singapore 1985.
- [5] K. Bräuer, A. Faessler, F. Fernández, K. Shimizu, *Z. Phys.* **A320**, 609 (1985).
- [6] K. Bräuer, A. Faessler, F. Fernández, K. Shimizu, *Nucl. Phys.* **A507**, 599 (1990).
- [7] K. Shimizu, *Rep. Progr. Phys.* **52**, 1 (1989).
- [8] E.V. Shuryak, *Phys. Rep.* **115**, 151 (1984).
- [9] D.I. Diakonov, V.Yu. Petrov, M. Prassalowicz, *Nucl. Phys.* **B323**, 53 (1989).
- [10] F. Fernández, A. Valcarce, U. Straub, A. Faessler, *J. Phys. G* **19**, 2013 (1993).
- [11] A. Valcarce, A. Buchmann, F. Fernández, A. Faessler, *Phys. Rev.* **C50**, 2246 (1994).
- [12] Z. Zhang, A. Faessler, U. Straub, L. Glozman, *Nucl. Phys.* **A578**, 573 (1994).
- [13] A. Valcarce, A. Buchmann, F. Fernández, A. Faessler, *Phys. Rev.* **C51**, 1480 (1995).
- [14] I.T. Obukhosky, A.M. Kusainov, *Phys. Lett.* **B238**, 142 (1990).
- [15] A.M. Kusainov, V.G. Neudatschin, I.T. Obukhosky, *Phys. Rev.* **C44**, 2343 (1991).
- [16] M.D. Scadron, *Phys. Rev.* **D26**, 239 (1982).

- [17] A. Buchmann, H. Ito, Y. Yamauchi, A. Faessler, *J. Phys. G* **14**, 1037 (1988).
- [18] Y. Yamauchi, A. Buchmann, A. Faessler, *Nucl. Phys.* **A494**, 401 (1989).
- [19] A. Buchmann, Y. Yamauchi, A. Faessler, *Nucl. Phys.* **A496**, 621 (1989).
- [20] Y. Yamauchi, A. Buchmann, A. Faessler, A. Arima, *Nucl. Phys.* **A526**, 495 (1991).
- [21] A. Buchmann, E. Hernández, K. Yazaki, *Phys. Lett.* **B269**, 35 (1991).
- [22] A. Valcarce, A. Faessler, F. Fernández, *Phys. Lett.* **B345**, 367 (1995).
- [23] R. Arndt *et al.*, *Phys. Rev.* **D45**, 3995 (1992).